Efficient Method of Optimizing Reverberation Chamber Using FDTD and Genetic Algorithm Method

Yao Z. Cui, Guang H. Wei, Song Wang, and Li S. Fan

Institute of Electrostatic and Electromagnetic Protection
Mechanical Engineering College, Shijiazhuang, 050003, China
cuiyaozhongcui@163.com, wei-guanghui@sohu.com, wangsongde@gmail.com, fanlisi@189.cn

Abstract **–** An efficient method combining the finite-difference time-domain (FDTD) method and genetic algorithm (GA) is proposed for the reverberation chamber (RC) optimization. In this method, the GA is utilized to optimize the parameters of RC model built by the FDTD method, such as the stirrer position and stirrer shape. Since the application of GA in the RC optimization and the RC model is automatically varied along with the optimization process, this method improves the accuracy and efficiency of the RC optimization. In addition, the influence of transmitting antenna position on the field uniformity around the lowest usable frequency is also investigated by this method. This method has been verified by comparing with the experiment results.

Index Terms **–** Field uniformity, finite-difference time-domain, genetic algorithm, reverberation chamber, stirrer, and transmitting antenna.

I. INTRODUCTION

The reverberation chamber (RC) is an electrically large and highly conductive enclosed cavity used for electromagnetic compatibility (EMC) measurements. Mechanical stirring is the most common technique used in the RC in order to produce fields that are statistically uniform and isotropic, and is accomplished by using rotating stirrers, which are made up of metal paddles inside the chamber. Consequently, the stirrer plays a key role in defining the RC performance. More precisely, the field uniformity inside the chamber can be enhanced by optimizing the stirrer position and stirrer shape. In [1], the optimization of the stirrer shape is investigated to improve the field uniformity of the RC. In [2, 3], the optimal stirrer position is found by studying the influence of different stirrer positions on the field uniformity of the RC. However, the optimal stirrer shape in [1] is chosen from the finite stirrer shapes given by the authors, and the optimal stirrer position in [2, 3] is chosen in the same way. Thus, since the optimization mechanism is artificial selection, the accuracy of the optimization results is limited, and the really optimal stirrer shape or the stirrer position may not be precise.

In order to improve the optimization accuracy, an efficient RC optimization method is proposed in this paper, which combines the FDTD method with the genetic algorithm (GA). Based on the standard deviation of the electric filed inside the RC, the GA is utilized to optimize the parameters of the RC model built by the FDTD method, such as the stirrer position and stirrer shape; thereby the optimization accuracy is improved. Furthermore, this method makes the RC model automatically varied along with the optimization process, which saves time and workload. In addition, the eigenmode density (number of modes per frequency interval) is low and the performance of the RC is not good when the RC operates around the lowest usable frequency (LUF) [4]. The transmitting antenna position will also slightly affect the performance of the RC, but there is less attention to this point. In this contribution, the influence of transmitting antenna position on the field uniformity around the LUF is also investigated by using our proposed method.

Submitted On: Nov. 14, 2012
Accepted On: Feb. 6, 2013

II. MODELING OF REVERBERATION CHAMBER

Numerical modeling of the RC is a very useful tool to analyze the electric field. The obvious goal of the simulation would be the complete design, evaluation, and optimization of the RC until all target specifications are met prior to physical construction. The RC test systems are designed to cover a broad frequency range. For a broad simulation response, frequency-domain methods, such as the method of moments (MoM) [5, 6] and the finite element method (FEM) [7], are at a disadvantage compared to time-domain methods such as FDTD [8, 9], the finite-volume time-domain (FVTD) [10], and the transmission line matrix (TLM) method [11]. While the latter requires only one simulation run to calculate the field in a large frequency band with the use of a Fourier transform, the former necessitate one simulation at each frequency point.

After evaluating the pros and cons of different numerical methods, we use the 3-D FDTD method as it is suited to the determination of all resonance frequencies and field properties in a frequency band. The RC model in this study is a rectangular cavity with dimensions 10.5 m × 8.0 m × 4.3 m (length × width × height), which is identical with the prototype RC. The first resonance frequency of the RC with this size is 24 MHz, and the LUF can be evaluated by multiplying the first resonance frequency by a constant whose value varies between 3 and 6 [12, 13]. Hence, the LUF of the RC analyzed in this paper is between 72 MHz and 144 MHz. Since the performance of the RC is poor around the LUF, it is of interest to optimize the performance of the RC around the LUF. Therefore, we have chosen to study the frequency band from 80 MHz to 150 MHz. The transmitting antenna model is a log-periodic operating between 60 MHz to 2 GHz, and a Gaussian pulse up to 300 MHz in the frequency domain is excited by this antenna. According to the FDTD principles defined in [14], the space and time increments are set equal to Δh = 0.1 m and $\Delta t = 1.7\times10^{-10}$ s, respectively (the space step is assumed to be the same for the three directions). In order to reduce the simulation time, an ideal wall is considered and air losses can be used to replace wall losses [8]. For the RC in this paper, the conductivity of the air is $\sigma = 2\times10^{-5}$ S/m obtained from the experimental analysis, and 25,000 time steps are needed to ensure that the FDTD algorithm converges to the steady state. In Fig. 1 the temporal electric field z-component signal (x = 5.0 m, y = 6.9 m, z = 2.15 m) reaches the equilibrium after 25,000 time steps.

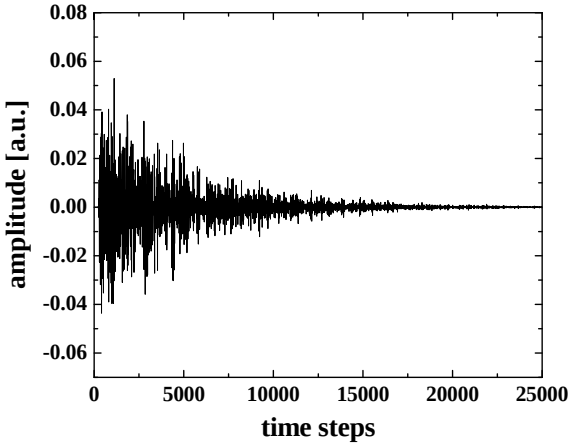

Fig. 1. Temporal electric field z-component signal inside the RC.

Figure 2 shows the internal structure of the prototype RC, with a log-periodic antenna, the horizontal stirrer, and the vertical stirrer. Since fifty angle positions may be required for the lower frequencies according to [15], the model needs to run fifty separate times for each investigated stirrer. The horizontal and vertical stirrers are stepped in fifty positions (10 × 5) in interleaved mode in this paper.

Fig. 2. Photo of the reverberation chamber prototype, showing a part of the horizontal stirrer on the right, the vertical stirrer, and a log-periodic transmitting antenna.

III. OPTIMIZATION PROCESS

Many empirical criteria and the classical statistical laws characterizing the RC electrical behavior have been proposed to ensure satisfactory functioning of the RC [16-20]. The standard deviation measurement is usually used to evaluate the field uniformity [15, 19]. In this case, the standard deviation σ_r (with $r = x, y, z$) of the eight maximal values over a stirrer rotation of each field component ($E_{r\max}$) calculated at eight points within the working volume, and the standard deviation σ_{24} of $E_{r\max}$ of three field components (24 values) are calculated, respectively (a more detailed presentation of calculating the standard deviation can be found in [15]). According to the norm IEC61000-4-21 [15], the smaller the standard deviation is, the better the field uniformity is. Furthermore, the σ is much easier to be used to evaluate the performance of the RC, since comparing several sets of graphs by eye, such as those depicted in Fig. 3, is very difficult. Hence, the σ_x, σ_y, σ_z and σ_{24} are taken as the objective functions, and the σ is defined as the average standard deviation over frequencies 80 MHz – 150 MHz in this paper.

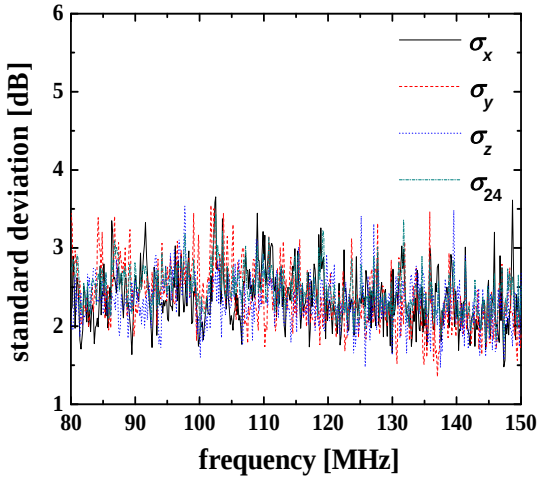

Fig. 3. Standard deviation of the RC model.

By letting the fitness function $F = \sigma_x + \sigma_y + \sigma_z + \sigma_{24}$, the multi-objective optimization problem becomes a single-object problem. Again, the field uniformity is getting better with the decrease of F. The GA is used to optimize the field uniformity of the RC model. The specific optimization process is as follows: (1) Generating an initial population of the optimization variables defining the transmitting antenna position (the stirrers shape or the stirrer position). The population size is 30. (2) Every individual of the optimization variable is assigned to the RC model, and the model is calculated by the FDTD method. (3) Calculating the fitness function F. (4) Selection takes place, where a stochastic universal sampling (SUS) is applied to select the quality individuals. (5) Crossover is followed, where a uniform crossover is applied to make individuals matched pairs in a crossover probability P_c that is 0.8. (6) Mutation, Gaussian mutation is applied to make the selected individuals stochastically vary gene in a mutation probability P_m that is 0.1. (7) The condition of termination; if the generation t is less than the maximum generation 30, program jumps to step number (2), or else the individual with the minimum fitness is exported.

It should be noted that the RC model is automatically modified by the program after the optimization variable is assigned to the RC model, which saves time and workload.

IV. OPTIMIZATION RESULTS

The transmitting antenna position, the stirrer shape, and the stirrer position are optimized by using our proposed method, respectively. The optimization variable is set as follows: (1) The coordinates of the transmitting antenna tail $x = a$, $y = b$, $z = c$, are the optimization variables when the antenna position is optimized, as shown in Fig. 4. (2) The angle φ and θ between the paddles are the optimization variables when the stirrer shape is optimized, as shown in Fig. 4. (3) The distance d_1 between the horizontal stirrer and the right wall of the chamber is the optimization variable when the stirrer position is optimized, as shown in Fig. 5 (N.B. the reason why the horizontal stirrer position is only optimized is that the vertical stirrer takes too much space and has to keep a distance from the transmitting antenna, so the range of the vertical stirrer position is small). (4) The a, b, c, φ, θ, and d_1 are the optimization variables when the global RC is optimized.

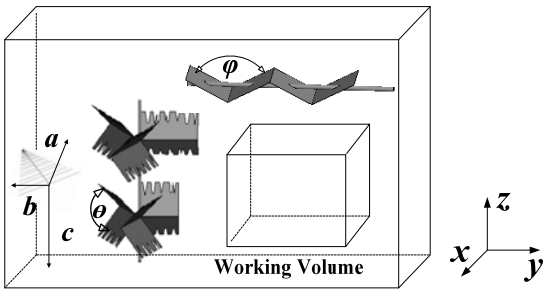

Fig. 4. Drawing of the RC model showing the horizontal stirrer with 'V' angle φ on the right, the vertical stirrer on the left with '<' angle θ and the transmitting antenna. The $x = a$, $y = b$, $z = c$, are the coordinates of the transmitting antenna tail. The working volume is $x \in [2.9, 7.0]$; $y \in [4.3, 9.5]$; $z \in [1.0, 3.3]$.

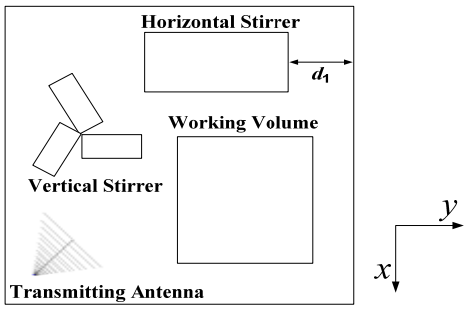

Fig. 5. Platform of the RC model, where d_1 is the distance between the horizontal stirrer and the right wall of the chamber.

Table 1 contains the optimal values of the optimization variables. From Table 1, it can be seen that the optimal values of the optimization variables when optimizing the global chamber are different from the optimal values when optimizing the transmitting antenna position, the stirrer shape and the stirrer position independently, which shows that the optimal values of these parameters are interactional.

It is well known that the stirrer shape and the stirrer position affect the field uniformity of the RC. However, as shown in Fig. 6, the transmitting antenna position also affects the field uniformity around the LUF, but relatively slightly compared with the stirrer shape and the stirrer position.

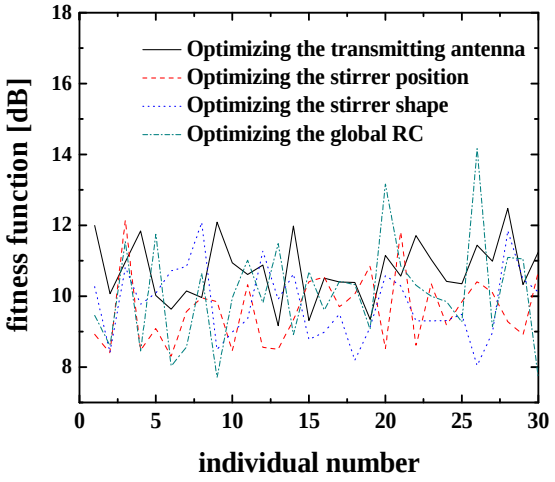

Fig. 6. Fitness functions versus individual number of the first generation.

Table 2 shows the optimization results. The results in Table 2 verify that the optimization improves the field uniformity of RC, but the improvement is small by optimizing the transmitting antenna position, and a much greater improvement in field uniformity is achieved by optimizing the stirrer position or the stirrer shape, which shows that the field distribution inside the RC is more sensitive to the stirrer.

Table 1: Optimal and initial values of the optimization variables.

	a/m	b/m	c/m	d_1/m	φ/°	θ/°
Initial	5.72	2.20	1.13	1.20	128.30	90.00
Optimal antenna position	6.43	2.43	1.87	—	—	—
Optimal stirrer position	—	—	—	4.25	—	—
Optimal stirrer shape	—	—	—	—	168.23	146.54
Optimal the global RC	6.35	2.26	2.08	3.33	127.48	161.62

Table 2: Optimization results.

	σ_x/dB	σ_y/dB	σ_z/dB	σ_{24}/dB	F/dB
Initial	2.35	2.37	2.30	2.46	9.48
Optimal antenna position	2.33	2.31	2.27	2.32	9.23
Optimal stirrer position	2.19	2.21	2.17	2.17	8.74
Optimal stirrer shape	2.16	2.15	2.14	2.18	8.63
Optimal the global RC	2.09	2.07	2.10	2.12	8.38

V. VERIFICATION OF THE OPTIMIZATION METHOD

The optimization method is verified by optimizing the transmitting antenna position to save the experiment resource. The field uniformity of the RC (see Fig. 1) is measured separately when the transmitting antenna is at initial and optimal positions. The horizontal and vertical stirrers are moved in 10 × 5 positions, in interleaved mode, using a stepper motor that is controlled by computer software. An optical fiber transmission field strength meter EMR-200 produced by Narda STS is used to measure the electric fields at the eight positions within the working volume.

Table 3 shows the standard deviation obtained from the measurement data for both the optimal and the initial position of the transmitting antenna. There is an improvement of 0.17 in the value of F between the optimal and the initial transmitting antenna position, which shows that the optimization does improve the field uniformity of the RC although, the modeled optimization results predicted a slightly larger improvement of 0.25 (see Table 2). The differences between the simulation and experiment results can be explained by the numerical dispersion of the FDTD scheme. Moreover, the differences could be reduced by using a more accurate mesh.

In addition, from the optimization results separately obtained by experiment and simulation (see Tables 2 and 3), we can note that, although the optimization does improve the RC's performance, the margin of improvement is not excessive by modifying only those six parameters (a, b, c, d_1, φ, and θ), especially the transmitting antenna position. Using this optimization method proposed in this paper, a much greater improvement in performance could be achieved by modifying more complex parameters that affect the design of the stirrer, rather than keeping the basic shape the same and searching for the best angles.

Table 3: Optimal and initial transmitting antenna position measurement results.

	σ_x/dB	σ_y/dB	σ_z/dB	σ_{24}/dB	F/dB
Initial	2.23	2.27	2.19	2.30	8.99
Optimal	2.17	2.18	2.23	2.24	8.82

VI. CONCLUSION

By applying the GA in the RC optimization design, an efficient RC optimization method is presented which improves the RC optimization accuracy and saves time and workload. Measurements have been performed to verify that the optimization within the GA does actually produce an improvement within a real chamber. The optimization results of simulation and experiment show that the field uniformity of the RC has been improved by optimizing the transmitting antenna position, the stirrer shape and the stirrer position, and the improvement obtained by optimizing the stirrer is larger compared with optimizing the transmitting antenna position.

Although the optimization does improve the RC's performance, the improvement is small by modifying only those six simple parameters (a, b, c, d_1, φ, and θ). As we all know, the larger the rotation volume of stirrer and the more complex the stirrer structure, the better the RC's performance. Consequently, in the future work, on the basis of the constant working volume, some more complex parameters that affect the design of the stirrer (e.g., the rotation volume and structure of the stirrer) could be optimized by using the

optimization method proposed in this paper, instead of keeping the basic shape the same and searching for the best angles.

In addition, since the performance of the RC is poor around the LUF, the performance of the RC around the LUF (from 80 MHz to 150 MHz) is investigated in this paper. When the RC operates around the higher frequency of the RC, the RC's performance will also be improved by optimization, but the improvement will be relatively small since the eigenmode density is high and the RC's performance is inherently good at high frequency. Consequently, it is of small significance to optimize the RC at high frequency.

REFERENCES

[1] J. I. Hong and C. S. Huh, "Optimization of stirrer with various parameters in reverberation chamber," *Progress In Electromagnetic Research*, vol. 104, pp. 15-30, 2010.

[2] L. Bai, L. Wang, B. Wang, and J. Song, "Effects of paddle configurations on the uniformity of the reverberation chamber," *IEEE Int. Symp. Electromagnetic Compatibility*, Seattle, WA, pp. 12-16, 1999.

[3] D. Zhang and J. Song, "Impact of stirrers' position on the properties of a reverberation chamber with two stirrers," *IEEE Int. Symp. Electromagnetic Compatibility*, Washington, DC, pp. 7-10, 2000.

[4] M. L. Crawford and G. H. Koepke, "Design, evaluation and use of a reverberation chamber for performing electromagnetic susceptibility /vulnerability measurements," *NBS Technical note 1092*, 1986.

[5] G. Freyer, T. Lehman, J. Ladbury, G. Koepke, and M. Hatfield, "Verification of fields applied to an EUT in a reverberation chamber using statistical theory," *IEEE Int. Symp. Electromagnetic Compatibility*, Denver, CO, pp. 34-38, 1998.

[6] C. Bruns and R. Vahldieck, "A closer look at reverberation chambers-3-D simulation and experimental verification," *IEEE Trans. Electromagn. Compat.*, vol. 47, no. 3, pp. 612-626, 2005.

[7] C. F. Bunting, "Statistical characterization and the simulation of a reverberation chamber using finite-element techniques," *IEEE Trans. Electromagn. Compat.*, vol. 44, no. 1, pp. 214-221, 2002.

[8] F. Moglie and V. M. Primiani, "Reverberation chambers: Full 3D FDTD simulations and measurements of independent positions of the stirrers," *IEEE Int. Symp. Electromagnetic Compatibility*, Rome,Italy, pp. 226-230, 2011.

[9] G. Orjubin, F. Petit, E. Richalot, S. Mengue, and O. Picon, "Cavity losses modeling using lossless FDTD method," *IEEE Trans. Electromagn. Compat.*, vol. 48, no. 2, pp. 429-431, 2006.

[10] F. Paladian, F. Diouf, S. Girard, P. Bonnet, and S. Lallechere, "Evaluation of FVTD dissipation and time-domain hybridization for MSRC studies," *23rd Annual Review of Progress in Applied Computational Electromagnetics (ACES)*, Verona, Italy, March 2007.

[11] A. Coates, H. G. Sasse, D. E. Coleby, A. P. Duffy, and A. Orlandi, "Validation of a three-dimensional transmission line matrix (TLM) model implementation of a mode-stirred reverberation chamber," *IEEE Trans. Electromagn. Compat.*, vol. 49, no. 4, pp. 734-744, 2007.

[12] M. Hatfield, M. Slocum, E. Godfrey, and G. Freyer, "Investigations to extend the lower frequency limit of reverberation chambers," *IEEE Int. Symp. Electromagnetic Compatibility*, Denver, CO, pp. 20-23, 1998.

[13] A. K. Mitra and T. F. Trost, "Statistical simulations and measurements inside a microwave reverberation chamber," *IEEE Int. Symp. Electromagnetic Compatibility*, Austin, TX, pp. 48-53, 1997.

[14] A. F. Peterson, S. L. Ray, and R. Mittra, *Computational Methods for Electromagnetics*, IEEE Press New York, 1998.

[15] *Electromagnetic Compatibility (EMC) - Part 4-21: Testing and measurement techniques - Reverberation Chamber Test Methods*, International Electrotechincal Commission, IEC61000-4-21 Draft, 2003.

[16] F. Moglie and V. M. Primiani, "Analysis of the independent positions of reverberation chamber stirrers as a function of their operating conditions," *IEEE Trans. Electromagn. Compat.*, vol. 53, no. 2, pp. 288-295, 2011.

[17] S. Mengué, E. Richalot, and O. Picon, "Comparison between different criteria for evaluating reverberation chamber functioning using a 3-D FDTD algorithm," *IEEE Trans. Electromagn. Compat.*, vol. 50, no. 2, pp. 237-245, 2008.

[18] C. Lemoine, P. Besnier, and M. Drissi, "Investigation of reverberation chamber measurements through high-power goodness-of-fit tests," *IEEE Trans. Electromagn. Compat.*, vol. 49, no. 4, pp. 745-755, 2007.

[19] N. Kouveliotis, P. Trakadas, and C. Capsalis, "Examination of field uniformity in vibrating intrinsic reverberation chamber using the FDTD method," *Electronics Lett.*, vol. 38, no. 3, pp. 109-110, 2002.

[20] D. A. Hill, “Plane wave integral representation for fields in reverberation chambers,” *IEEE Trans. Electromagn. Compat.*, vol. 40, no. 3, pp. 209-217, 1998.

Yaozhong Cui was born in Hebei province, China, in 1986. He received the B.Eng. from Xidian University, Shanxi, China, in 2008, the M.Eng. from Mechanical Engineering College, Shijiazhuang, China, in 2010. He is currently working toward the Ph.D. degree at Mechanical Engineering College, Shijiazhuang, China. His research interests include computational electromagnetic and electromagnetic measurement in reverberation chamber.

Guanghui Wei was born in Hebei province, China, in 1964. He received the B.Sc. and the M. Sc. Degree from Nankai University, Tianjin, China in 1984 and 1987, respectively. He is Professor of Institute of Electrostatic and Electromagnetic Protection at the Mechanical Engineering College. His research interests include computational electromagnetic, EMC test environments and EMC measurement techniques.

Song Wang was born in Hebei province, China, in 1987. He received the B.Sc. from Beihang University, Beijing, China, in 2010. He is currently working toward the Ph.D. degree at Mechanical Engineering College, Shijiazhuang, China. His research interests include computational electromagnetic and electromagnetic measurement in reverberation chamber.